International Journal of Innovative Computing, Information and Control
Volume **16**, Number **2**, April **2020**
ICIC International ©2020 ISSN 1349-4198
pp. 749–764

ADAPTIVE DYNAMIC SURFACE CONTROL FOR HIGHER-ORDER MODELS OF SYNCHRONOUS GENERATORS

Adirak Kanchanaharuthai[1] and Ekkachai Mujjalinvimut[2]

[1]Department of Electrical Engineering
Rangsit University
52/347 Muang-Ake, Phaholyothin Road, Lak-Hok, Muang, Patumthai 12000, Thailand
adirak@rsu.ac.th

[2]Department of Electrical Engineering
Faculty of Engineering
King Mongkut's University of Technology Thonburi
Pracha Uthit Road, Bang Mod, Bangkok 10140, Thailand
ekkachai.muj@kmutt.ac.th

Received September 2019; revised January 2020

Abstract. *An adaptive dynamic surface controller (DSC) scheme for higher-order models of synchronous generators in the presence of unknown parameters is presented in this paper. In spite of the presence of unknown parameters in the system models, the developed control law is used to stabilize the closed-loop system and avoid the problem of "explosion of terms" inherent in backstepping approach. Further, with the help of Lyapunov stability arguments, the proposed control scheme can guarantee that all trajectories of the overall closed-loop dynamics are semi-globally uniformly ultimately bounded. The simulation results exhibit the effectiveness of the proposed control strategy. It can offer excellent dynamic performance, avoid the problem of backstepping complexity explosion, and perform better than a conventional adaptive backstepping control design.*
Keywords: Higher-order model, Adaptive dynamic surface control, Generator excitation control, Adaptive control

1. **Introduction.** It is well-known that maintaining power system stability and operations is one of the most challenging tasks in power systems once faced with inevitable disturbances. Recently, there are many interests in this problem [1-3] in the literature. Because of an increase of the size and complexity in modern power systems, power systems become highly nonlinear and more complicated. When there are increased load demands, system stability may operate close to stability limits. This may decrease the stability margin of the overall system and is unstable eventually. As a result, feedback stabilizing nonlinear control algorithms used to alleviate adverse or undesired effects from disturbances should be studied. The use of excitation control of synchronous generators plays a significant role in maintaining power system stability and operations. There are currently several researchers [5-11] focusing on the design of excitation control techniques to maintain and enhance power system stability. There has so far been the only one-axis model of synchronous generators used in the design procedure of the references above, while automatic voltage regulation (AVR) dynamics are ignored. Kanchanaharuthai [12] proposed a method to add the dynamics of the direct-axis transient voltage E'_d for enhancing the control performance. This inclusion can increase greater flexibility for the system

DOI: 10.24507/ijicic.16.02.749

stability enhancement. Moreover, this way can include degree of freedoms to figure out the effective control due to the use of both d-axis and q-axis field windings.

To the best of authors' knowledge, the nonlinear design control using both d-axis and q-axis models (higher-order models) of synchronous generators including the dynamics of AVR was presented in [13, 14]. By means of adaptive backstepping design, an adaptive excitation control [13] for transient stability enhancement and voltage regulation of the fifth-order models of synchronous generators was proposed. The resulting controller performed better than the adaptive design for the third-order models. Orchi et al. [14] proposed a partial feedback linearing model predictve excitation control for the two-axis models of synchronous generators together with the dynamics of IEEE Type-II excitation system in multi-machine power systems. Although there were different operating conditions in the system, the obtained controller can maintain the dynamic stability. With the help of a combination of backstepping-like control and nonlinear disturbance observer, a composite nonlinear control [15] was presented to enhance the dynamic control performances and reject the adverse effects of unavoidable disturbances, simultaneously.

In practice, there are always unknown parameters/uncertainties in most engineering systems. Such unknown parameters may unavoidably degrade the desired control performances of the system of interest. Therefore, if it is possible, the results of unknown parameters should be estimated and compensated by an inclusion of additional dynamics, in particular adaptation law dynamics, into the whole system. A parameter estimate scheme [16] has been widely used to compensate or reject the adverse effects arising from unknown parameters effectively. This technique has been extensively employed to compensate the effects of unknown parameters and find out parameter estimation dynamics. Moreover, this method can be combined with backstepping control design [16] to improve the control performances and to mitigate the undesired effect of unknown parameters simultaneously. Also, it can be successfully applied for numerous kinds of real engineering systems. For power systems, the robust adaptive backstepping excitation control for a single-machine infinite bus (SMIB) power system reported in [13] worked well and offered good desired control performances. Mitra et al. [17] developed an adaptive backstepping control approach to design a generator excitation control for SMIB power systems. In the work, the damping coefficient was considered as unknown parameters. A robust adaptive excitation control [18] for multi-machine power systems under parametric uncertainties and external disturbances was proposed for transient stability enhancement. Roy et al. [19, 20] presented a robust adaptive backstepping excitation control for multi-machine power systems where the damping coefficient, d- and q-axes open-circuit transient constants, transient reactance, and external disturbances.

Motivated by these abovementioned works, although adaptive backstepping method is a powerful method for control design and successfully applicable for power systems and several real systems, it has an important drawback. This drawback is the problem of "explosion of complexity" and comes from the evaluations of the repeated differentiations of virtual control functions. It often occurs in large-scale systems, resulting in a difficulty in computing the time derivative of the virtual control functions in each design step. This makes the final control law more complicated. In order to avoid this disadvantage, a concept of dynamic surface control design [21, 22] to eliminate the problem of repeated differentiations of the virtual control variables is presented. In addition, this approach can be extended to adaptive control to deal with the explosion of terms arising inherent in adaptive backstepping.

In this paper, a systematic strategy to design an adaptive dynamic surface controller for higher-order models of synchronous generators [22] is developed to deal with the problem of "explosion of terms". Also, in the higher-order models of power systems, a variety of important unknown parameters of particular interest are damping coefficient, inertia constant, d- and q-axes open-circuit transient constants, and transient reactance. Therefore, the main contributions of this paper can be summarized as follows: (i) An adaptive dynamic surface controller for transient stability enhancement and voltage regulation of the higher-order (fifth-order) models of power systems in the presence of unknown parameters has not been investigated before; (ii) Despite the presence of unknown parameters, the developed control law is designed to guarantee that all signals of the overall closed-loop system are semi-globally uniformly ultimately bounded; and (iii) Compared with a conventional adaptive backstepping control, the developed control law offers good dynamic performances and can avoid computing the problem of "explosion of complexity".

The rest of this paper is organized as follows. A dynamic model of a higher-order model of synchronous generators is briefly presented, and the problem statement is given in Section 2. Controller design is developed in Section 3 while simulation results are mentioned in Section 4. Finally, in Section 5, a conclusion is given.

Remark 1.1. *Although this paper focuses on the design of adaptive dynamic surface control for a single-machine infinite bus power system, a practical application of the higher-order models of synchronous generators is how the developed scheme performs when applied to large-scale power systems in the presence of external disturbances. As a result, the proposed control needs to be further extended for multi-machine power systems that will be studied in the future.*

2. Power System Model Description.

The two-axis model of synchronous generators along with the dynamics of an IEEE ST1 standard exciter or IEEE Type-II exciter [1, 23] is considered in this paper. Thus, the complete dynamical model of the synchronous generator connected to an infinite bus with the IEEE Type II excitation system can be expressed as follows:

$$\begin{cases} \dot{\delta} = \omega - \omega_s \\ \dot{\omega} = \dfrac{\omega_s}{2H}\left(P_m - E'_q I_q - E'_d I_d - (X'_d - X'_q) I_d I_q - D(\omega - \omega_s)\right) \\ \dot{E}'_q = \dfrac{1}{T'_{d0}}\left(-E'_q + (X_d - X'_d) I_d + E_{fd}\right) \\ \dot{E}'_d = \dfrac{1}{T'_{q0}}\left(-E'_d - \left(X_q - X'_q\right) I_q\right) \\ \dot{E}_{fd} = -\dfrac{E_{fd}}{T_A} + \dfrac{K_A}{T_A}(V_{ref} - V_t + u_c) \end{cases} \tag{1}$$

with $I_d = \frac{V_\infty \cos\delta - E'_q}{X'_{d\Sigma}}$, $I_q = \frac{E'_d - V_\infty \sin\delta}{X'_{q\Sigma}}$, where δ is the power angle of the generator, ω denotes the relative speed of the generator, $D \geq 0$ is a damping constant, and E'_q and E'_d are the field variable proportional to field flux linkages and the damper variable proportional to the d-axis damaper flux linkages, respectively. E_{fd} is the equivalent field excitation voltage. X'_d and X'_q are the d-axis and q-axis transient reactances, respectively. P_e is the electrical power delivered by the generator to the voltage at the infinite bus V_∞, ω_s is the synchronous machine speed, $\omega_s = 2\pi f$, H represents the per unit inertial constant, and f is the system frequency. $X'_{d\Sigma} = X'_d + X_T + X_L$ is the reactance consisting of the direct axis transient reactance of SG, the reactance of the transformer, and the reactance of the transmission line X_L. $X'_{q\Sigma}$ denotes the q-axis reactances. T'_{d0} and T'_{q0} are the d-axis and q-axis transient open-circuit time constants. u_c is the stabilizing signal which is the control input to be designed, respectively. T_A is the time constant of the voltage regulator connected to the synchronous generator. K_A is the gain of the voltage regulator connected to the synchronous generator. V_t and V_{ref} denote the terminal voltage of synchronous generators and the reference terminal voltage, respectively. I_d and I_q denote the d- and q-axes current components, respectively.

Remark 2.1. *In addition to the practical application mentioned in Remark 1.1, it is observed that the dynamics of two-axis model of synchronous generators consists of practically unmeasurable state variables such as E'_q and E'_d. This is a practically important issue that needs to be addressed. In cope with this issue, the output feedback controller should be studied. Therefore, throughout this paper, for simplicity we assume that all of state variables in (1) are measurable and used to design the desired control law.*

For convenience, let us define new state variables as follows:

$$x_1 = \delta - \delta_e, \quad x_2 = \omega - \omega_s, \quad x_3 = E'_q, \quad x_4 = E'_d, \quad x_5 = E_{fd} \tag{2}$$

Subsequently, after differentiating the state variables (2), the higher-order model of synchronous generators can be expressed in the following form of an affine nonlinear system[1]:

$$\dot{x} = f(x) + g(x)u(x) \tag{3}$$

where

$$\begin{cases} f(x) = \begin{bmatrix} f_1(x) \\ f_2(x) \\ f_3(x) \\ f_4(x) \\ f_5(x) \end{bmatrix} = \begin{bmatrix} x_2 \\ \theta_D x_2 + \theta_\omega P_m + \theta_d x_3 \sin(x_1 + \delta_0) \\ +\theta_q x_4 \cos(x_1 + \delta_0) + \theta_m \sin 2(x_1 + \delta_0) \\ \theta_1 x_3 + \theta_2 \cos(x_1 + \delta_e) + \theta_3 x_5 \\ \theta_4 x_4 + \theta_5 \sin(x_1 + \delta_e) \\ \theta_6 x_5 + \theta_7 (V_{ref} - V_t) \end{bmatrix} \\ g(x) = \begin{bmatrix} 0 \\ 0 \\ 0 \\ 0 \\ \theta_2 \end{bmatrix}, \quad u(x) = u_c \end{cases} \tag{4}$$

where $\theta_D = -\frac{\omega_s}{2H}D$, $\theta_\omega = \frac{\omega_s}{2H}$, $\theta_d = \frac{V_\infty}{X'_{d\Sigma}}$, $\theta_q = \frac{V_\infty}{X'_{q\Sigma}}$, $\theta_m = \frac{X'_{d\Sigma} - X'_{q\Sigma}}{2X'_{d\Sigma}X'_{q\Sigma}}$, $\theta_1 = -\frac{X_{d\Sigma}}{X'_{d\Sigma}T'_{d0}}$, $\theta_2 = \frac{(X_{d\Sigma} - X'_{d\Sigma})}{X'_{d\Sigma}T'_{d0}}V_\infty$, $\theta_3 = \frac{1}{T'_{d0}}$, $\theta_4 = -\frac{X_{q\Sigma}}{X'_{q\Sigma}T'_{q0}}$, $\theta_5 = \frac{(X_{q\Sigma} - X'_{q\Sigma})}{X'_{q\Sigma}T'_{q0}}V_\infty$, $\theta_6 = -\frac{1}{T_A}$, $\theta_7 = \frac{K_A}{T_A}$. The region of operation is defined in the set $\mathcal{D} = \left\{x \in \mathcal{S} \times \mathbb{R} \times \mathbb{R} \times \mathbb{R} \times \mathbb{R} \middle| \, 0 < x_1 < \frac{\pi}{2}\right\}$. The open loop operating equilibrium is denoted by $x_0 = [0,\ 0,\ x_{30},\ x_{40},\ x_{50}]^T = \left[0,\ 0,\ E'_{q0},\ E'_{d0},\ E_{fd0}\right]^T$. For the sake of simplicity, the power system considering (3) and (4) can be expressed as follows.

$$\begin{cases} \dot{x}_1 = x_2 \\ \dot{x}_2 = \theta_D x_2 + \theta_\omega P_m + \theta_d x_3 \sin(x_1 + \delta_0) + \theta_q x_4 \cos(x_1 + \delta_0) + \theta_m \sin 2(x_1 + \delta_0) \\ \dot{x}_3 = \theta_1 x_3 + \theta_2 \cos(x_1 + \delta_0) + \theta_3 x_5 \\ \dot{x}_4 = \theta_4 x_4 + \theta_5 \sin(x_1 + \delta_0) \\ \dot{x}_5 = \theta_6 x_5 + \theta_7 (V_{ref} - V_t + u_c) \end{cases} \tag{5}$$

[1]It is assumed that all functions and mappings are $\mathbb{C}^\infty$ throughout this paper.

In real applications, unknown parameters always appear in the system model. In power system stability analysis, there are two practical parameters which cannot measure accurately and are often unknown. One is a damping coefficient [24] in a synchronous generator model. The other is an unknown mechanical input power or a sudden mechanical perturbation that is important uncertainties in the power system. Therefore, both parameters need to be real-time estimated; otherwise, they may destabilize the power system stability and operations. For instance, it is evident that after the mechanical power is perturbed to a new constant value. It makes the equilibrium of the system shifted to a new corresponding point. In practice, if the unknown perturbation in mechanical power occurs [25-28], the new operating point will be unknown as well.

For notational convenience, let us define $\theta = [\theta_D, \theta_\omega, \theta_d, \theta_q, \theta_m, \theta_1, \theta_2, \theta_3, \theta_4, \theta_5, \theta_6, \theta_7]^T$ as unknown constant parameters in (5).

Problem statement: The control objective of this paper is to solve the problem of the stabilization of the system (5) including unknown parameters θ, which can be formulated as follows: using dynamic surface strategy, we design an adaptive control law $u(x)$ and parameter estimation $\hat{\theta}$ as follows:

$$u = \phi\left(x, \hat{\theta}\right), \quad \dot{\hat{\theta}} = \varphi\left(x, u, \hat{\theta}\right) \tag{6}$$

such that all trajectories of the overall closed-loop system (5) and (6) are semi-globally uniformly and ultimately bounded, where $\hat{\theta}$ is the estimate of θ.

3. **Adaptive DSC Design and Stability Analysis.**

In this section, the desired control law for stabilizing the higher models of synchronous generators in the presence of unknown parameters is developed. To accomplish the main control development, the proposed design procedure consists of two subsections: (i) The first subsection is to use a dynamic surface control scheme to find out an adaptive control law capable of stabilizing the closed-loop system and identifying online the unknown parameters of the system; (ii) In the second subsection, with the help of Lyapunov stability arguments, the stability analysis of the overall closed-loop dynamics is shown to ensure that all state variables are semi-globally uniformly ultimately bounded despite the presence of unknown parameters.

3.1. **Adaptive DSC design.**

The proposed control procedure is developed step by step as follows.

Step 1: First, let us define the first error surface $S_1 = x_1$, and the time derivative of S_1 is defined as $\dot{S}_1 = x_2$, then a Lyapunov function candidate is chosen as

$$V_1 = \frac{1}{2}S_1^2 \tag{7}$$

The time derivative of V_1 along the system trajectories becomes

$$\dot{V}_1 = S_1\dot{S}_1 = S_1x_2 \tag{8}$$

Assume that x_2 is a virtual control variable corresponding to the dynamics of a rotor angle tracking error or the first subsystem of (5) to drive S_1 to zero:

$$\alpha_1 = -c_1S_1 \tag{9}$$

where c_1 is a positive design parameter. Let us introduce a new state variable x_{2d} and let α_1 pass through a first-order filter with time constant τ_2 to obtain x_{2d}

$$\tau_2\dot{x}_{2d} + x_{2d} = \alpha_1, \quad x_{2d}(0) = \alpha_1(0) \Rightarrow \dot{x}_{2d} = -\frac{e_2}{\tau_2} \tag{10}$$

where $e_2 = x_{2d} - \alpha_1$ is the boundary layer error.

Step 2: Define the second surface as $S_2 = x_2 - x_{2d}$. Then, we choose the Lyapunov function candidate as

$$V_2 = \frac{1}{2}S_1^2 + \frac{1}{2\rho_D}\tilde{\theta}_D^2 + \frac{1}{2\rho_\omega}\tilde{\theta}_\omega^2 + \frac{1}{2\rho_d}\tilde{\theta}_d^2 + \frac{1}{2\rho_q}\tilde{\theta}_q^2 + \frac{1}{2\rho_m}\tilde{\theta}_m^2 \tag{11}$$

where $\tilde{\theta}_l = \theta_l - \hat{\theta}_l$ $(l = D, \omega, d, q, m)$ denotes the estimation errors corresponding to the known parameters θ_l. $\hat{\theta}_l$ is the estimated value of θ_l. ρ_l are positive constants. By calculating the derivative of (11), we have

$$\begin{aligned}
\dot{V}_2 &= S_2\left(\dot{x}_2 - \dot{x}_{2d}\right) - \frac{\tilde{\theta}_D\dot{\hat{\theta}}_D}{\rho_D} - \frac{\tilde{\theta}_\omega\dot{\hat{\theta}}_\omega}{\rho_\omega} - \frac{\tilde{\theta}_d\dot{\hat{\theta}}_d}{\rho_d} - \frac{\tilde{\theta}_q\dot{\hat{\theta}}_q}{\rho_q} - \frac{\tilde{\theta}_m\dot{\hat{\theta}}_m}{\rho_m} \\
&= S_2\Big(\left(\hat{\theta}_D + \tilde{\theta}_D\right)x_2 + \left(\hat{\theta}_\omega + \tilde{\theta}_\omega\right)P_m + \left(\tilde{\theta}_d + \hat{\theta}_d\right)x_3\sin(x_1+\delta_0) \\
&\quad + \left(\tilde{\theta}_q + \hat{\theta}_q\right)x_4\cos(x_1+\delta_0) + \left(\tilde{\theta}_m + \hat{\theta}_m\right)\sin 2(x_1+\delta_0) - \dot{x}_{2d}\Big) \\
&\quad - \frac{\tilde{\theta}_D\dot{\hat{\theta}}_D}{\rho_D} - \frac{\tilde{\theta}_\theta\dot{\hat{\theta}}_\omega}{\rho_\omega} - \frac{\tilde{\theta}_d\dot{\hat{\theta}}_d}{\rho_d} - \frac{\tilde{\theta}_q\dot{\hat{\theta}}_q}{\rho_q} - \frac{\tilde{\theta}_m\dot{\hat{\theta}}_m}{\rho_m} \\
&= S_2\left(\hat{\theta}_D x_2 + \hat{\theta}_\omega P_m + \hat{\theta}_d x_3\sin(x_1+\delta_0) + \hat{\theta}_q x_4\cos(x_1+\delta_0) + \hat{\theta}_m\sin 2(x_1+\delta_0) - \dot{x}_{2d}\right) \\
&\quad + \left(S_2x_2 - \frac{\dot{\hat{\theta}}_D}{\rho_D}\right)\tilde{\theta}_D + \left(S_2P_m - \frac{\dot{\hat{\theta}}_\omega}{\rho_\omega}\right)\tilde{\theta}_\omega + \left(S_2x_3\sin(x_1+\delta_0) - \frac{\dot{\hat{\theta}}_d}{\rho_d}\right)\tilde{\theta}_d \\
&\quad + \left(S_2x_4\cos(x_1+\delta_0) - \frac{\dot{\hat{\theta}}_q}{\rho_q}\right)\tilde{\theta}_q + \left(S_2\sin 2(x_1+\delta_0) - \frac{\dot{\hat{\theta}}_m}{\rho_m}\right)\tilde{\theta}_m
\end{aligned} \tag{12}$$

Choose two virtual control variables α_2 and α_3 to drive $S_2 \to 0$, $S_3 \to 0$ as follows:

$$\begin{cases}
\alpha_2 = -\dfrac{1}{\hat{\theta}_d\sin(x_1+\delta_0)}\left(\hat{\theta}_\omega P_m + \dfrac{1}{2}\left(c_2S_2 - \dot{x}_{2d} + \hat{\theta}_D x_2 + \hat{\theta}_m\sin 2(x_1+\delta_0)\right)\right) \\
\alpha_3 = -\dfrac{1}{2\hat{\theta}_q\cos(x_1+\delta_0)}\left(c_2S_2 - \dot{x}_{2d} + \hat{\theta}_D x_2 + \hat{\theta}_m\sin 2(x_1+\delta_0)\right)
\end{cases} \tag{13}$$

where c_2 is a positive constant. Once again, let us introduce two new state variables x_{3d} and x_{4d}; therefore, we pass α_2 and α_3 through two first-order filters, with time constants (τ_3, τ_4) to obtain x_{3d} and x_{4d}, respectively,

$$\begin{cases}
\tau_3\dot{x}_{3d} + x_{3d} = \alpha_2, \quad x_{3d}(0) = \alpha_2(0) \Rightarrow \dot{x}_{3d} = -\dfrac{e_3}{\tau_3} \\
\tau_4\dot{x}_{4d} + x_{4d} = \alpha_3, \quad x_{4d}(0) = \alpha_3(0) \Rightarrow \dot{x}_{4d} = -\dfrac{e_4}{\tau_4}
\end{cases} \tag{14}$$

where $e_3 = x_{3d} - \alpha_2$ and $e_4 = x_{4d} - \alpha_3$ denote the boundary layer errors.

Moreover, in this step we have the update laws for the parameter estimation as follows:

$$\begin{cases}
\dot{\hat{\theta}}_D = \rho_D S_2 x_2 - k_D\hat{\theta}_D \\
\dot{\hat{\theta}}_\omega = \rho_\omega S_2 P_m - k_\omega\hat{\theta}_\omega \\
\dot{\hat{\theta}}_d = \rho_d(S_2x_3 - (S_3 + e_3))\sin(x_1+\delta_0) - k_d\hat{\theta}_d \\
\dot{\hat{\theta}}_q = \rho_q(S_2x_4 - (S_4 + e_4))\cos(x_1+\delta_0) - k_q\hat{\theta}_q \\
\dot{\hat{\theta}}_m = \rho_m S_2\sin 2(x_1+\delta_0) - k_m\hat{\theta}_m
\end{cases} \tag{15}$$

where k_D, k_ω, k_d, k_q and k_m are positive design parameters.

Step 3: Let us define the third and the fourth surfaces to be $S_3 = x_3 - x_{3d}$ and $S_4 = x_4 - x_{4d}$. Then, the Lyapunov function candidate is chosen as

$$V_3 = \frac{1}{2}S_3^2 + \frac{1}{2}S_4^2 + \sum_{i=1}^{5} \frac{1}{2\rho_i}\tilde{\theta}_i^2 \tag{16}$$

where $\tilde{\theta}_i = \theta_i - \hat{\theta}_i$, $(i = 1, 2, 3, 4)$ denotes the estimation errors corresponding to the known parameters θ_i. $\hat{\theta}_i$ is the estimated value of θ_i. ρ_i is a positive constant.

Then the time derivative of V_3 along the system trajectories turns into as follows:

$$\begin{aligned}
\dot{V}_3 &= S_3\left(\dot{x}_3 - \dot{x}_{3d}\right) + S_4\left(\dot{x}_4 - \dot{x}_{4d}\right) - \sum_{i=1}^{5}\frac{\dot{\hat{\theta}}_i\tilde{\theta}_i}{\rho_i} \\
&= S_3\left(\hat{\theta}_1 x_3 + \hat{\theta}_2\cos(x_1+\delta_0) + \hat{\theta}_3 x_5 - \dot{x}_{3d}\right) + S_4\left(\hat{\theta}_4 x_4 + \hat{\theta}_5\sin(x_1+\delta_0) - \dot{x}_{4d}\right) \\
&\quad + \tilde{\theta}_1\left(S_3x_3 - \frac{\dot{\hat{\theta}}_1}{\rho_1}\right) + \tilde{\theta}_2\left(S_3\cos(x_1+\delta_0) - \frac{\dot{\hat{\theta}}_2}{\rho_2}\right) + \tilde{\theta}_3\left(S_3x_5 - \frac{\dot{\hat{\theta}}_3}{\rho_3}\right) \\
&\quad + \tilde{\theta}_4\left(S_4x_4 - \frac{\dot{\hat{\theta}}_4}{\rho_4}\right) + \tilde{\theta}_5\left(S_4\cos(x_1+\delta_0) - \frac{\dot{\hat{\theta}}_5}{\rho_5}\right)
\end{aligned} \tag{17}$$

From (17), it is easy to choose a virtual control to driven $S_3 \to 0$,

$$\alpha_4 = -\frac{1}{\hat{\theta}_3}\left(c_3S_3 + \hat{\theta}_1x_3 + \hat{\theta}_2\cos(x_1+\delta_0) - \dot{x}_{3d}\right) \tag{18}$$

Furthermore, it is essential from (17) to obtain the following expression:

$$\hat{\theta}_4x_4 + \hat{\theta}_5\sin(x_1+\delta_0) - \dot{x}_{4d} = -c_4S_4 \tag{19}$$

Once again, let us introduce a new state variable x_{5d}; thus, we pass α_4 through a first-order filter, with time constant (τ_4) to obtain x_5 as follows:

$$\tau_5\dot{x}_{5d} + x_{5d} = \alpha_4, \quad x_{5d}(0) = \alpha_4(0) \Rightarrow \dot{x}_{5d} = -\frac{e_5}{\tau_5} \tag{20}$$

where $e_5 = x_{5d} - \alpha_4$ is the boundary layer error.

Moreover, for this step, the update laws for the parameter estimation are as follows:

$$\begin{cases}
\dot{\hat{\theta}}_1 = \rho_1S_3x_3 - k_1\hat{\theta}_1 \\
\dot{\hat{\theta}}_2 = \rho_2S_3\cos(x_1+\delta_0) - k_2\hat{\theta}_2 \\
\dot{\hat{\theta}}_3 = \rho_3(S_3x_5 - (S_5+e_5)) - k_3\hat{\theta}_3 \\
\dot{\hat{\theta}}_4 = \rho_4S_4x_4 - k_4\hat{\theta}_4 \\
\dot{\hat{\theta}}_5 = \rho_5S_4\sin(x_1+\delta_0) - k_5\hat{\theta}_5
\end{cases} \tag{21}$$

where k_1, k_2, k_3, k_4, k_5 are positive design parameters.

Step 4: Let us define the surface as $S_5 = x_5 - x_{5d}$. Similarly, let us introduce the Lyapunov function as

$$V_4 = \frac{1}{2}S_5^2 + \sum_{j=1}^{7}\frac{1}{2\rho_j}\tilde{\theta}_j^2 \tag{22}$$

where $\tilde{\theta}_j = \theta_i - \hat{\theta}_j$, $(j = 6, 7)$ denotes the estimation errors corresponding to the known parameters θ_j. $\hat{\theta}_j$ is the estimated value of θ_j. ρ_j is a positive constant. Then the time derivative of V_4 along the system trajectories turns into as follows:

$$\begin{aligned}\dot{V}_4 &= S_5\left(\dot{x}_5 - \dot{x}_{5d}\right) - \sum_{j=6}^{7} \frac{\dot{\hat{\theta}}_j \tilde{\theta}_j}{\rho_j} \\ &= S_5\left(\hat{\theta}_6 x_5 + \hat{\theta}_7 (V_{ref} - V_t + u_c) - \dot{x}_{5d}\right) \\ &\quad + \tilde{\theta}_6 \left(S_5 x_5 - \frac{\dot{\hat{\theta}}_6}{\rho_6}\right) + \tilde{\theta}_7 \left(S_5 (V_{ref} - V_t + u_c) - \frac{\dot{\hat{\theta}}_7}{\rho_7}\right)\end{aligned} \tag{23}$$

Thus, a suitable control law u_c is selected as follows:

$$u_c = V_{ref} - V_t + \frac{1}{\hat{\theta}_7}\left(-c_5 S_5 + \dot{x}_{5d} - \hat{\theta}_6 x_5\right) \tag{24}$$

where c_5 is a positive design parameter. Apart from this, the update laws for the parameter estimate are the following:

$$\dot{\hat{\theta}}_6 = \rho_6 S_5 x_5 - k_6 \hat{\theta}_6, \quad \dot{\hat{\theta}}_7 = \rho_7 S_5 (V_{ref} - V_t + u_c) - k_7 \hat{\theta}_7 \tag{25}$$

where k_6 and k_7 are positive design parameters.

3.2. **Stability analysis.** In this subsection, the stability analysis for the presented scheme is studied. The objective of this part is to indicate that the closed-loop system has the semi-globally uniformly ultimate boundedness property. First, by subtracting and adding x_{kd}, and α_{k-1}, $(k = 2, 3, 4, 5)$ in x_l, $(l = 1, 2, 3, 4, 5)$, the dynamics of high-order models of synchronous generators can be rewritten as follows:

$$\begin{cases} \dot{x}_1 = x_2 - x_{2d} + x_{2d} - \alpha_1 + \alpha_1 = S_2 + e_2 - \alpha_1 = S_2 + e_2 - c_1 S_1 \\ \dot{x}_2 = \theta_D x_2 + \theta_\omega P_m + \theta_d (x_3 - x_{3d} + x_{3d} - \alpha_2 + \alpha_2) \sin(x_1 + \delta_0) \\ \qquad + \theta_q (x_4 - x_{4d} + x_{4d} - \alpha_3 + \alpha_3) \cos(x_1 + \delta_0) + \theta_m \sin 2(x_1 + \delta_0) \\ \quad = \theta_D x_2 + \theta_\omega P_m + \theta_d (S_3 + e_3 + \alpha_2) \sin(x_1 + \delta_0) + \theta_q (S_4 + e_4 + \alpha_3) \cos(x_1 + \delta_0) \\ \qquad + \theta_m \sin 2(x_1 + \delta_0) = -c_2 S_2 + \theta_d (S_3 + e_3) + \theta_q (S_4 + e_4) + \dot{x}_{2d} \\ \dot{x}_3 = -\theta_1 x_3 + \theta_2 I_d + \theta_3 (x_5 - x_{5d} + x_{5d} - \alpha_4 + \alpha_4) \\ \quad = -\theta_1 x_3 + \theta_2 I_d + \theta_3 (S_5 + e_5 + \alpha_4) = -c_3 S_3 + \theta_3 (S_5 + e_5) + \dot{x}_{3d} \\ \dot{x}_4 = -c_4 S_4 + \dot{x}_{4d}, \ \dot{x}_5 = -c_5 S_5 + \dot{x}_{5d} \end{cases} \tag{26}$$

where $S_l = x_l - x_{ld}$, $l = 1, 2, 3, 4, 5$, $x_{1d} = 0$ and $e_k = x_{kd} - \alpha_{k-1}$, $k = 2, 3, 4, 5$. Based on the definition of the surface errors, one has the time derivative of the surface errors as follows:

$$\begin{cases} \dot{S}_1 = -c_1 S_1 + S_2 + e_2 \\ \dot{S}_2 = -c_2 S_2 + \theta_d (S_3 + e_3) + \theta_q (S_4 + e_4) \\ \dot{S}_3 = -c_3 S_3 + \theta_3 (S_5 + e_5) \\ \dot{S}_4 = -c_4 S_4, \quad \dot{S}_5 = -c_5 S_5 \end{cases} \tag{27}$$

In addition, we need to consider the boundary errors because of the effect of inclusion of a set of the first-order low-pass filters. According to the definition of the boundary layer errors, we have the filter dynamics as follows:

$$\dot{e}_k = -\frac{e_k}{\tau_k} + B_k\left(S_1, \dots, S_k, e_2, \dots, e_k, \hat{\theta}_D, \dots, \hat{\theta}_5\right) \tag{28}$$

where $B_k(\cdot)$ is a continuous function defined as follows:

$$\begin{cases} B_2(\cdot) = -\dot{\alpha}_1 = -\dfrac{\partial\alpha_1}{\partial x_1}\dot{x}_1 \\ B_3(\cdot) = -\dot{\alpha}_2 = -\dfrac{\partial\alpha_2}{\partial x_1}\dot{x}_1 - \dfrac{\partial\alpha_2}{\partial x_2}\dot{x}_2 - \dfrac{\partial\alpha_2}{\partial\hat{\theta}_\omega}\dot{\hat{\theta}}_\omega - \dfrac{\partial\alpha_2}{\partial\hat{\theta}_D}\dot{\hat{\theta}}_D - \dfrac{\partial\alpha_2}{\partial\hat{\theta}_d}\dot{\hat{\theta}}_d - \dfrac{\partial\alpha_2}{\partial\hat{\theta}_m}\dot{\hat{\theta}}_m \\ B_4(\cdot) = -\dot{\alpha}_3 = -\dfrac{\partial\alpha_3}{\partial x_1}\dot{x}_1 - \dfrac{\partial\alpha_3}{\partial x_2}\dot{x}_2 - \dfrac{\partial\alpha_3}{\partial\hat{\theta}_\omega}\dot{\hat{\theta}}_\omega - \dfrac{\partial\alpha_3}{\partial\hat{\theta}_D}\dot{\hat{\theta}}_D - \dfrac{\partial\alpha_2}{\partial\hat{\theta}_q}\dot{\hat{\theta}}_q - \dfrac{\partial\alpha_2}{\partial\hat{\theta}_m}\dot{\hat{\theta}}_m \\ B_5(\cdot) = -\dot{\alpha}_4 = -\dfrac{\partial\alpha_4}{\partial x_1}\dot{x}_1 - \dfrac{\partial\alpha_4}{\partial x_3}\dot{x}_3 - \dfrac{\partial\alpha_4}{\partial\hat{\theta}_1}\dot{\hat{\theta}}_1 - \dfrac{\partial\alpha_4}{\partial\hat{\theta}_2}\dot{\hat{\theta}}_2 - \dfrac{\partial\alpha_4}{\partial\hat{\theta}_3}\dot{\hat{\theta}}_3 \end{cases} \tag{29}$$

Therefore, the main result of this work can be summarized in the following theorem.

Theorem 3.1. *Consider the closed-loop dynamics consisting of the higher-order model of synchronous generators (5), the control law (24), the parameter estimate algorithms (15), (21), (25), and linear filters (10), (14), (20). Assume that all state variables are measurable. If there exists a set of suitable design parameters* c_l, k_r, ρ_r, τ_k ($l = 1,2,3,4,5$, $r = D,\omega,d,q,m,1,2,3,4,5$, $k = 2,3,4,5$) *satisfying*

$$\begin{cases} \bar{c}_1 = c_1 - 1.5 \\ \bar{c}_2 = c_2 - \theta_d^2 - \theta_q^2 - 0.5 \\ \bar{c}_3 = c_3 - \theta_3^2 - 0.5 \\ \bar{c}_4 = c_4 - 0.5 \\ \bar{c}_5 = c_5 - 0.5 \\ \bar{c}_{k0} = \dfrac{1}{\tau_k} - \dfrac{\bar{B}_k^2}{2\pi_k} - \dfrac{1}{2}, \quad k_r > 0, \quad \rho_r > 0 \end{cases} \tag{30}$$

such that all signals of the overall closed-loop dynamics are semi-globally uniformly and ultimately bounded.

Proof: We define the Lynapunov function as

$$V = \sum_{j=1}^{4} V_j + \sum_{k=2}^{5} \frac{1}{2} e_k^2 \tag{31}$$

The time derivative of V along trajectories (27) and (28) is as follows:

$$\begin{aligned} \dot{V} &= \sum_{l=1}^{5} S_l\dot{S}_i - \tilde{\theta}_D\dot{\hat{\theta}}_D - \tilde{\theta}_\omega\dot{\hat{\theta}}_\omega - \tilde{\theta}_d\dot{\hat{\theta}}_d - \tilde{\theta}_q\dot{\hat{\theta}}_q - \tilde{\theta}_m\dot{\hat{\theta}}_m - \sum_{i=1}^{7}\tilde{\theta}_i\dot{\hat{\theta}}_i + \sum_{k=2}^{5} e_k\dot{e}_k \\ &= S_1(-c_1S_1 + S_2 + e_2) + S_2(-c_2S_2 + \theta_d(S_3 + e_3) + \theta_q(S_4 + e_4)) \\ &\quad + S_3(-c_3S_3 + \theta_3(S_5 + e_5)) - c_4S_4^2 - c_5S_5^2 + \frac{k_D}{\rho_D}\tilde{\theta}_D\dot{\hat{\theta}}_D + \frac{k_\omega}{\rho_\omega}\tilde{\theta}_\omega\dot{\hat{\theta}}_\omega + \frac{k_d}{\rho_d}\tilde{\theta}_d\dot{\hat{\theta}}_d \\ &\quad + \frac{k_q}{\rho_q}\tilde{\theta}_q\dot{\hat{\theta}}_q + \frac{k_m}{\rho_m}\tilde{\theta}_m\dot{\hat{\theta}}_m + \sum_{i=1}^{7}\frac{k_i}{\rho_i}\tilde{\theta}_i\dot{\hat{\theta}}_i + \sum_{k=2}^{5} e_k\left(-\frac{e_k}{\tau_k} + B_k\right) \end{aligned} \tag{32}$$

For $j = 1,2,3,4$, $k = 2,3,4,5$ and $p > 0$, the set $\Omega := \sum_{j=1}^{4} 2V_j + \sum_{k=2}^{5} e_k^2 \le 2p$ is compact set in R^{21}. According to the property of continuous function, we know that $B_k(\cdot)$

has a bound on Ω, such that $|B_k(\cdot)| \leq \bar{B}_k$, $k = 2, 3, 4, 5$. Based on the Young's inequality ($2ab \leq a^2 + b^2$), we have the following inequalities:

$$S_1S_2 \leq \frac{S_1^2}{2} + \frac{S_2^2}{2}, \quad S_1e_2 \leq \frac{S_1^2}{2} + \frac{e_2^2}{2}, \quad \theta_dS_2S_3 \leq \frac{(\theta_d)^2S_2^2}{2} + \frac{S_3^2}{2},$$
$$\theta_dS_2e_3 \leq \frac{(\theta_d)^2S_2^2}{2} + \frac{e_3^2}{2}, \quad \theta_qS_2S_4 \leq \frac{(\theta_q)^2S_2^2}{2} + \frac{S_4^2}{2}, \quad \theta_qS_2e_4 \leq \frac{(\theta_q)^2S_2^2}{2} + \frac{e_4^2}{2},$$
$$\theta_3S_3S_5 \leq \frac{\theta_3^2S_3^2}{2} + \frac{S_5^2}{2}, \quad \theta_3S_3e_5 \leq \frac{\theta_3^2S_3^2}{2} + \frac{e_5^2}{2},$$
$$e_k\left(-\frac{e_k}{\tau_k} + B_k\right) \leq -\left(\frac{1}{\tau_k} - \frac{\bar{B}_k^2}{2\pi_k}\right)e_k^2 + \frac{\pi_k}{2}, \quad \pi_k > 0, \quad k = 2, 3, 4, 5.$$

Note that

$$\frac{k_r}{\rho_r}\tilde{\theta}_r\hat{\theta}_r = \frac{k_r}{2\rho_r}\tilde{\theta}_r\left(\theta_r - \tilde{\theta}_r\right) \leq -\frac{k_r}{2\rho_r}\tilde{\theta}_r^2 + \frac{k_r}{2\rho_r}\theta_r^2, \quad r = D, \omega, d, q, m, 1, 2, \ldots, 7 \tag{33}$$

From the inequalities above, one has

$$\begin{aligned}\dot{V} &= -(c_1 - 1)S_1^2 - \left(c_2 - \theta_d^2 - \theta_q^2 - 0.5\right)S_2^2 - \left(c_3 - \theta_3^2 - 0.5\right)S_3^2 - (c_4 - 0.5)S_4^2 \\ &\quad -(c_5 - 0.5)S_5^2 \\ &\leq -\sum_{k=2}^{5}\left(\frac{1}{\tau_k} - \frac{\bar{B}_k^2}{2\pi_k} - \frac{1}{2}\right)e_k^2 - \frac{k_D}{2\rho_D}\tilde{\theta}_D^2 - \frac{k_\omega}{2\rho_\omega}\tilde{\theta}_\omega^2 - \frac{k_d}{2\rho_d}\tilde{\theta}_d^2 - \frac{k_q}{2\rho_q}\tilde{\theta}_q^2 - \frac{k_m}{2\rho_m}\tilde{\theta}_m^2 \\ &\quad -\sum_{i=1}^{7}\frac{k_i}{2\rho_i}\tilde{\theta}_i^2 + \Pi\end{aligned} \tag{34}$$

where $\Pi = \sum_{k=2}^{5}\frac{\pi_k}{2} + \frac{k_D}{2\rho_D}\theta_D^2 + \frac{k_\omega}{2\rho_\omega}\theta_\omega^2 + \frac{k_d}{2\rho_d}\theta_d^2 + \frac{k_q}{2\rho_q}\theta_q^2 + \frac{k_m}{2\rho_m}\theta_m^2 + \sum_{i=1}^{7}\frac{k_i}{2\rho_i}\theta_i^2$.

After selecting $c_1 = \bar{c}_1 + 1$, $c_2 = \bar{c}_2 + \theta_d^2 + \theta_q^2 + 0.5$, $c_3 = \bar{c}_3 + \theta_3^2 + 0.5$, $c_4 = \bar{c}_4 + 0.5$, $c_5 = \bar{c}_5 + 0.5$, $\frac{1}{\tau_k} = \bar{c}_{k0} + \frac{\bar{B}_k^2}{2\pi_k} + \frac{1}{2}$, we obtain

$$c = \min\left\{\bar{c}_1, \ldots, \bar{c}_5, \bar{c}_{20}, \ldots, \bar{c}_{50}, \frac{k_D}{2\rho_D}, \frac{k_\omega}{2\rho_\omega}, \frac{k_d}{2\rho_d}, \frac{k_q}{2\rho_q}, \frac{k_m}{2\rho_m}, \frac{k_1}{2\rho_1}, \ldots, \frac{k_5}{2\rho_5}\right\} > 0 \tag{35}$$

After that, the following inequalities hold.

$$\dot{V} \leq -cV + \Pi \tag{36}$$

After solving the inequality (36), we obtain

$$0 \leq V(t) \leq \left(V(0) - \frac{\Pi}{c}\right)e^{-ct} + \frac{\Pi}{c} \tag{37}$$

From (37), it can be inferred that $V(t)$ eventually settles down to $\frac{\Pi}{c}$. This means that all the trajectories of the closed-loop dynamics are semi-globally uniformly ultimately bounded. From (37), it is easy to know that V, S_l, e_k, and $\tilde{\theta}_r$ are bounded, and the closed-loop dynamics are stable. $\hat{\theta}_r = \theta_r - \tilde{\theta}_r$ are bounded due to the boundedness of θ_r and $\tilde{\theta}_r$. Because $S_l = x_l - x_{ld}$ are bounded, x_l are bounded as well. Similarly, α_{k-1} is a function of bounded signals S_l, $\hat{\theta}_r$ and x_{ld}, so α_{k-1} is also bounded. Also, it can be concluded that S_l, e_k, $\tilde{\theta}_r$, x_l, α_{k-1} are all bounded. In addition, since $V_{Sl} = \frac{1}{2}S_l^2$, one has

$$\sum_{l=1}^{5}\frac{1}{2}S_l^2 \leq V \tag{38}$$

From the inequality in (37), the following inequality holds:

$$\lim_{t \to +\infty} S_l \leq \sqrt{2V} \leq \sqrt{\frac{2\Pi}{c}} \tag{39}$$

It can be observed from (39) that the boundedness of the surface errors (S_l) depends upon a suitable selection of design parameters c_l, k_r, ρ_r, τ_k as given in (30). Further, based on appropriately tuning the design parameters, the surface errors can be regulated to an arbitrary small neighborhood of the desired equilibrium. This completes the proof.

Remark 3.1. *The novelty and the advantages of this paper over existing results are as follows: (i) The proposed control method is able to enhance transient stability and guarantee that all trajectories of the overall closed-loop dynamics are bounded; (ii) The developed control law is designed without directly finding the derivative of virtual control functions at each step; and (iii) The presented scheme provides satisfactory dynamic performances in spite of the presence of unknown parameters.*

4. **Simulation Results.** In this section, in order to verify the effectiveness of the proposed nonlinear controller. The proposed controller is evaluated via simulations of a single-machine infinite bus (SMIB) power system consisting of the fifth-order model of synchronous generators as shown in Figure 1. The performance of the proposed control scheme is evaluated in MATLAB environment.

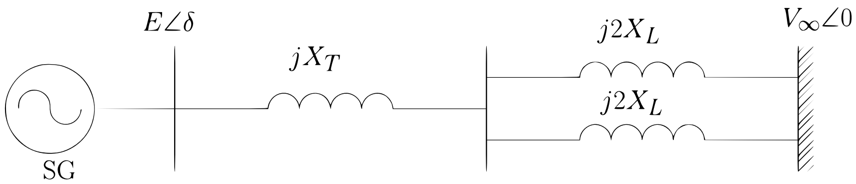

Figure 1. A single line diagram of SMIB model

The physical parameters (pu.), the controller parameters, and initial conditions used for this power system model are as follows.

- The actual parameter values of high-order model of synchronous generators and transmission line: $\omega_s = 2\pi f$ rad/s, $D = 5$, $H = 4$, $f = 60$ Hz, $T'_{d0} = 0.4$, $T'_{q0} = 0.1$, $V_\infty = 1\angle 0°$, $\omega = \omega_s$, $X_q = 1.7$, $X'_q = 0.28$, $X_d = 1.8$, $X'_d = 0.17$, $X_T = 0.1$, $X_L = 0.15$.
- The design parameters of the proposed controller are $c_l = 100$, $(l = 1, 2, 3, 4, 5)$, $k_r = 1$, $\rho_r = 10$, $(r = D, \omega, d, q, m, 1, 2, \ldots, 7)$, $\tau_k = 0.01$, $(k = 2, 3, 4, 5)$.
- Initial conditions $\delta_0 = 1.20135$ rad, $E'_{q0} = 0.4391$, $E'_{d0} = 0.703$, $E_{fd0} = 0.7422$, $x_{kd} = 0$, $(k = 2, 3, 4, 5)$.

For the simulations, assume that there is a symmetrical three-phase fault occurring at the point P as shown in Figure 1. For the fault of interest, there are five stages of interest as follows. Firstly, all state variables are at pre-fault steady state. The fault occurs at $t = 0.5$ sec. Afterwards, the fault is isolated by opening the breaker at $t = 0.7$ sec. The transmission line can be restored at $t = 1.5$ sec. Eventually, the system returns to a post-fault state.

The time domain simulations are carried out to investigate the system stability enhancement and the dynamic performance of the designed controller, as given in (24). To exhibit the control performance and the advantages of the proposed adaptive dynamic surface controller, a conventional adaptive backstepping controller (CABC) design [13] is employed for comparison, as given in (40):

$$u_{\text{cabc}} = V_t - V_{ref} - \frac{1}{\hat{\theta}_7}\left(c_5 z_5 + \theta_3 z_3 + \hat{\theta}_6 x_5 - \dot{\alpha}_4\right) \tag{40}$$

where $z_i = x_i - \alpha_{i-1}$, $i = 1,2,3,4,5$, $\alpha_0 = 0$, $\alpha_1 = -c_1 z_1$, $\alpha_2 = -\frac{1}{\hat{\theta}_d \sin(x_1+\delta_0)}\Big(\hat{\theta}_\omega P_m + 0.5\left(z_1 + \hat{\theta}_D x_2 + \hat{\theta}_m \sin 2(x_1+\delta_0) + c_2 z_2 - \dot{\alpha}_1\right)\Big)$, $\alpha_3 = -\frac{1}{2\hat{\theta}_q \cos(x_1+\delta_0)}\left(z_1 + \hat{\theta}_D x_2 + \hat{\theta}_m \sin 2(x_1+\delta_0) + c_2 z_2 - \dot{\alpha}_1\right)$, $\alpha_4 = -\frac{1}{\hat{\theta}_3}\left(c_3 z_3 + z_2 \hat{\theta}_d \sin(x_1+\delta_0) + \hat{\theta}_1 x_3 + \hat{\theta}_2 \cos(x_1+\delta_0) - \dot{\alpha}_2\right)$, $\dot{\hat{\theta}}_D = \rho_D z_2 x_2 - k_D \hat{\theta}_D$, $\dot{\hat{\theta}}_\omega = \rho_\omega z_2 P_m - k_\omega \hat{\theta}_\omega$, $\dot{\hat{\theta}}_d = \rho_d z_2 (x_3 + z_3)\sin(x_1+\delta_0) - k_d \hat{\theta}_d$, $\dot{\hat{\theta}}_q = \rho_q z_2 (x_4 + z_4)\cos(x_1+\delta_0) - k_q \hat{\theta}_q$, $\dot{\hat{\theta}}_m = \rho_m z_2 \sin 2(x_1+\delta_0) - k_m \hat{\theta}_m$, $\dot{\hat{\theta}}_1 = \rho_1 z_3 x_3 - k_1 \hat{\theta}_1$, $\dot{\hat{\theta}}_2 = \rho_2 z_2 \cos(x_1+\delta_0) - k_2 \hat{\theta}_2$, $\dot{\hat{\theta}}_3 = \rho_3 z_3 (x_5 + z_5) - k_3 \hat{\theta}_3$, $\dot{\hat{\theta}}_4 = \rho_4 z_4 x_4 - k_4 \hat{\theta}_4$, $\dot{\hat{\theta}}_5 = \rho_5 z_4 \cos(x_1+\delta_0) - k_5 \hat{\theta}_5$, $\dot{\hat{\theta}}_6 = \rho_6 z_5 x_5 - k_6 \hat{\theta}_6$, $\dot{\hat{\theta}}_7 = \rho_7 z_2 (V_{ref} - V_t + u_{\text{cabc}}) - k_7 \hat{\theta}_7$. The controller parameters of this scheme are set as $c_i = 100$, $(i = 1,2,3,4,5)$, $k_r = 1$, $\rho_r = 10$, $r = D, \omega, d, q, m, 1, 2, \ldots, 7$.

Remark 4.1. *It is evident from (40) that the obtained control law depends on computing the repeated differentiations of the virtual control functions $(\alpha_1, \alpha_2, \alpha_3, \alpha_4)$ in each design step. Therefore, this computation makes the design procedure more complicated as compared with the proposed control (24).*

The simulation results are presented and discussed as follows. Time histories of the power angle, frequency, d-axis and q-axis transient internal voltages along with field voltage under two controllers are presented in Figures 2 and 3, respectively.

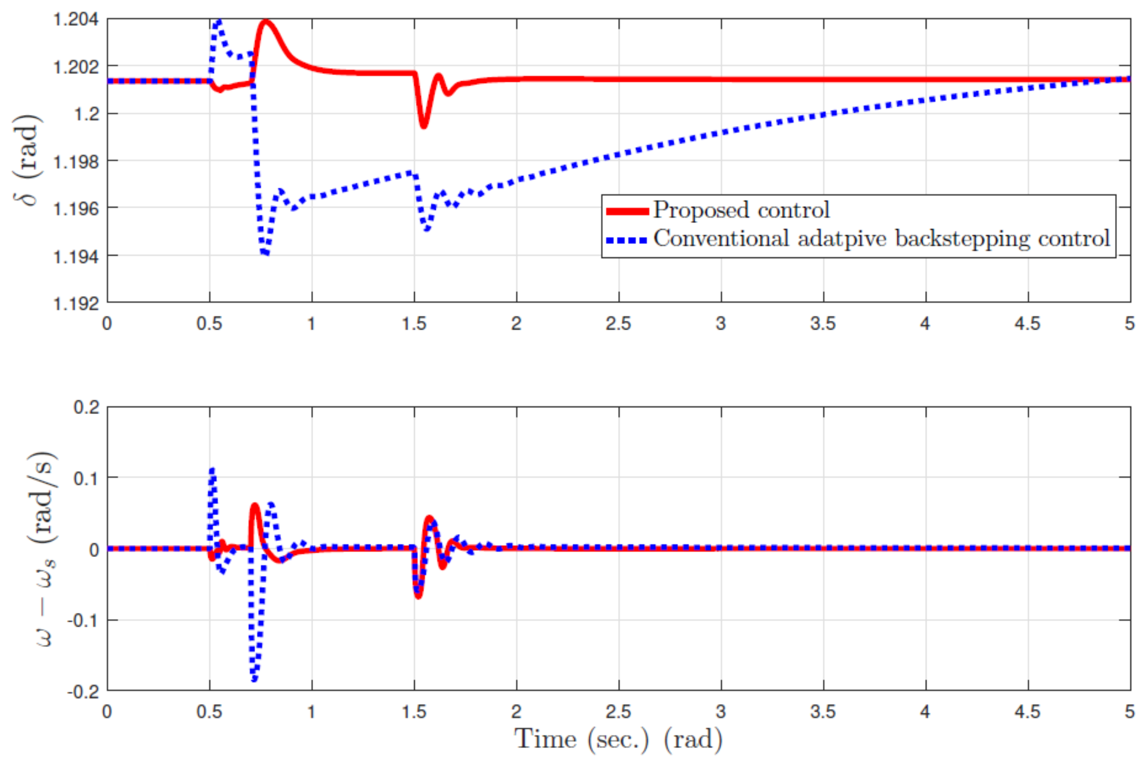

FIGURE 2. Controller performance – Power angles (δ) (rad.), and frequency $(\omega - \omega_s)$ rad/s (Solid: Proposed control, Dotted: Conventional adaptive backstepping control)

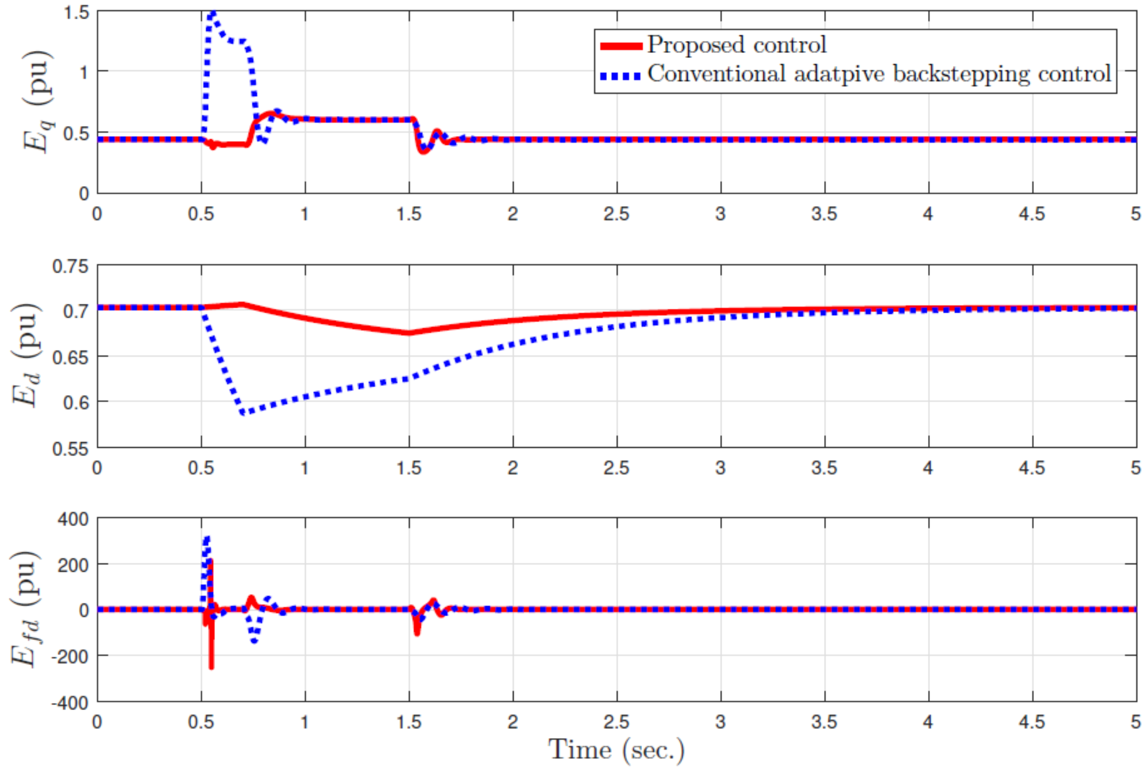

FIGURE 3. Controller performance – The q-axis transient internal voltage (E_q) (pu.) and the d-axis transient internal voltage (E_d) (pu.) and field voltage (E_{fd}) (Solid: Proposed control, Dotted: Conventional adaptive backstepping control)

It can be seen from these figures that the presented design and the CBSC design can settle down to the desired equilibrium point. Clearly, the developed scheme can reach better transient performances such as a shorter settling time, a short rise time, and a faster convergence rate. In contrast, all time responses are sluggishly damped by the CABC approach. In comparison with the CBSC method, the presented controller offers a good dynamic performance such as satisfactory overshoots and rapidly suppressing oscillations. Figures 4 and 5 show the parameter estimators $\left(\hat{\theta}_r\right)$ can settle down to their pre-fault values after the fault is isolated. This shows the effectiveness and superiority of the developed control capable of estimating unknown parameters successfully.

From the simulation results above, it is obvious that after the proposed approach is applied to the SMIB power systems, it offers the advantages over the CABC method as follows.

- Although the proposed controller can steer all trajectories of closed-loop dynamics to the equilibrium rapidly like the CABC method, it is not necessary to compute the time derivative of the virtual control functions in each design step. This eventually enables us to avoid the problem of "explosion of complexity" inherent in backstepping.
- The developed control strategy can guarantee that the states of closed-loop system are semi-globally uniformly ultimately bounded. It also provides better superior transient performances. In particular, it can be seen that the dynamic responses of the presented control are improved as compared with the CABC method in spite of having unknown parameters.

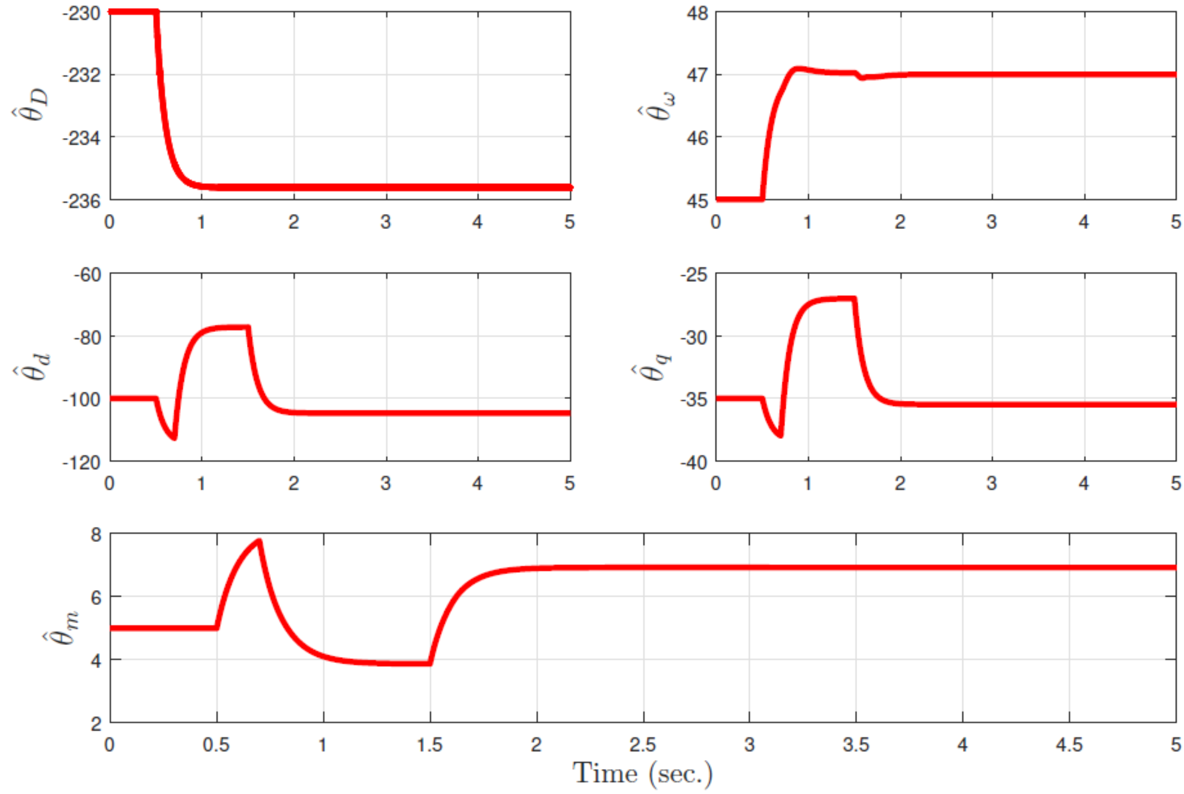

FIGURE 4. Parameter estimations: $\hat{\theta}_D$, $\hat{\theta}_\omega$, $\hat{\theta}_d$, $\hat{\theta}_q$, and $\hat{\theta}_m$

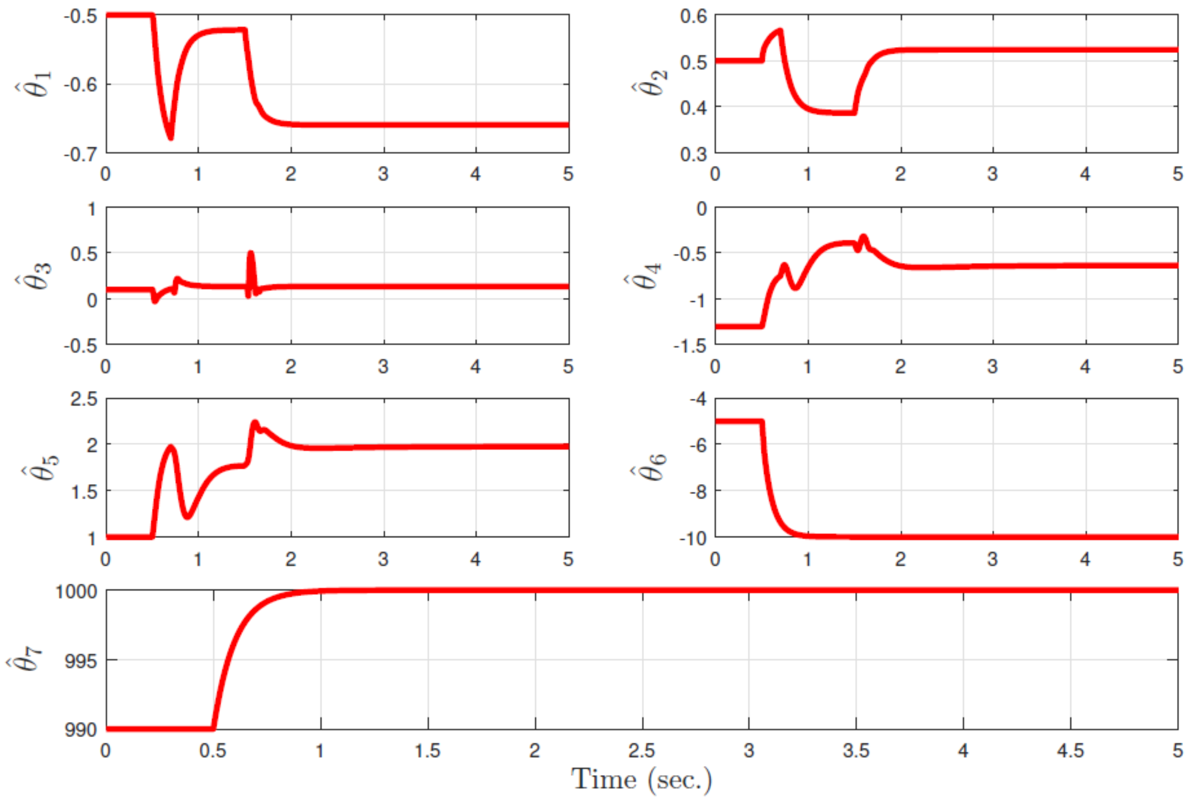

FIGURE 5. Parameter estimations: $\hat{\theta}_1$, $\hat{\theta}_2$, $\hat{\theta}_3$, $\hat{\theta}_4$, $\hat{\theta}_5$, $\hat{\theta}_6$ and $\hat{\theta}_7$

5. **Conclusion.** In this paper, an adaptive control scheme for higher-order models of synchronous generators in the presence of unknown parameters has been presented. The proposed strategy has been developed via a dynamic surface control approach. This p-resented design procedure can offer better transient performance and avoid the problem of "explosion of terms" inherent in backstepping approach as compared with the conventional adaptive backstepping control (CABC). With the help of Lyapunov control theory, the stability analysis of closed-loop system has been provided to guarantee that all signals of the overall closed-loop dynamics are semi-globally uniformly ultimately bounded. The simulation results have confirmed the effectiveness and superiority of the proposed method over the CABC method. The future study will focus on the extension of this approach to an adaptive dynamic surface controller for multi-machine power systems in the presence of external disturbances. In addition, an adaptive dynamic surface control combined with fuzzy approximation [29] for multi-machine power systems will be investigated in the future.

REFERENCES

[1] P. Kundur, *Power System Stability and Control*, McGraw-Hill, 1994.

[2] P. W. Sauer and M. A. Pai, *Power System Dynamics and Stability*, Stipes Publishing L.L.C, 1997.

[3] K. R. Padiyar, *Power System Dynamics: Stability and Control*, Anshan Limited, 2002.

[4] A. S. Bazanella and C. L. Conceicao, Transient stability improvement through excitation control, *International Journal of Robust and Nonlinear Control*, vol.14, pp.891-910, 2004.

[5] M. Galaz-Larios, R. Ortega, A. S. Bazanella and A. M. Stankovic, An energy-shaping approach to excitation control of synchronous generators, *Automatica*, vol.39, pp.111-119, 2003.

[6] R. Ortega, M. Galaz, A. Astolfi, Y. Sun and T. Shen, Transient stabilization of multi-machine power systems with nontrivial transfer conductances, *IEEE Trans. Automatic Control*, vol.50, pp.60-75, 2005.

[7] M. O. Paul and E. P. Gerardo, Output feedback excitation control of synchronous generators, *International Journal of Robust and Nonlinear Control*, vol.14, pp.879-890, 2004.

[8] H. Liu, Z. Hu and Y. Song, Lyapunov-based decentralized excitation control for global asymptotical stability and voltage regulation of multi-machine power systems, *IEEE Trans. Power Systems*, vol.27, pp.2262-2270, 2012.

[9] Y. Liu, Q. H. Wu and X. X. Zhou, Coordinated switching controllers for transient stability of multi-machine power systems, *IEEE Trans. Power Systems*, vol.31, pp.3937-3949, 2016.

[10] Q. Lu, Y. Sun and S. Wei, *Nonlinear Control Systems and Power System Dynamics*, Kluwer Academic Publishers, Boston, 2001.

[11] W. Dib, R. Ortega and D. J. Hill, Transient stability enhancement of multi-machine power system: Synchronization via immersion of a pendular system, *Asian Journal of Control*, vol.15, no.4, p.19, 2013.

[12] A. Kanchanaharuthai, Immersion and invariance-based nonlinear dual-excitation and steam-valving control of synchronous generators, *International Trans. Electrical Energy Systems*, vol.24, no.12, pp.1671-1687, 2014.

[13] T. K. Roy, M. A. Mahmud, A. M. T. Oo and H. R. Pota, Nonlinear adatptive backstepping excitation controller design for higher-order models of synchronous generators, *The 20th IFAC World Congress.*, pp.4368-4373, 2017.

[14] T. F. Orchi, T. K. Roy, M. A. Mahmud and A. M. T. Oo, Feedback linearizing model predictive excitation controller design for multimachine power systems, *IEEE Access*, vol.6, pp.2310-2319, 2018.

[15] A. Kanchanaharuthai and E. Mujjalinvimut, A composite nonlinear controller for higher-order models of synchronous generators under external disturbances, *International Journal of Innovative Computing, Information and Control*, vol.15, no.2, pp.465-478, 2019.

[16] M. Krstic, I. Kanellakopoulos and P. V. Kokotivic, *Nonlinear and Adaptive Control Design*, John Willey & Sons, 1995.

[17] A. Mitra, M. Mukherjee and K. Naik, Enhancement of power system transient stability using a novel adaptive backstepping control law, *Proc. of the 3rd International Conference on Computer, Communication, Control and Information Technology (C3IT)*, Hooghly, pp.1-5, 2015.

[18] T. K. Roy, M. A. Mahmud, A. M. T. Oo and M. E. Haque, Robust adaptive excitation control of synchronous generators in multimachine power systems under parametric uncertainties and external disturbances, *IEEE Proc. of the 56th Annual Conference Decision and Control*, pp.2655-2660, 2017.
[19] T. K. Roy, M. A. Mahmud and A. M. T. Oo, Robust adaptive backstepping excitation controller design for higher-order models of synchronous generators in multimachine power systems, *IEEE Trans. Power Systems*, vol.34, no.1, pp.40-51, 2019.
[20] T. K. Roy, M. A. Mahmud, W. Shen and A. M. T. Oo, Nonlinear adaptive excitation controller design for multimachine power systems with unknown stability sensitive parameters, *IEEE Trans. Control Systems Technology*, vol.25, no.6, pp.2060-2072, 2017.
[21] D. Swaroop, J. K. Hedrick, P. P. Yip and J. C. Gerdes, Dynamic surface control for a class of nonlinear systems, *IEEE Trans. Automatic Control*, vol.45, no.10, pp.1893-1899, 2000.
[22] P. P. Yip and J. K. Hedrick, Adaptive dynamic surface control: A simplified algorithm for adaptive backstepping control of nonlinear systems, *International Journal of Control*, vol.71, no.5, pp.959-979, 1998.
[23] M. A. Mahmud, M. J. Hossain, H. R. Pota and A. M. T. Oo, Robust partial feedback linearizing excitation controller design for multimachine power systems, *IEEE Trans. Power Systems*, vol.32, no.1, pp.3-16, 2017.
[24] W. Hu, S. Mei, Q. Lu, T. Shen and A. Yokoyama, Nonlinear adaptive decentralized stabilizing control of multi-machine systems, *Applied Mathematics and Computation*, vol.133, pp.519-532, 2002.
[25] G. Damm, R. Marino and F. Lamnabhi-Lagarrigue, Adaptive nonlinear output feedback for transient stabilization and voltage regulation of power generators with unknown parameters, *International Journal of Robust and Nonlinear Control*, vol.14, pp.833-855, 2004.
[26] T. K. Roy, M. A. Mahmud, W. Shen and A. M. T. Oo, Nonlinear adaptive excitation controller design for multi-machine power systems, *Proc. of 2015 IEEE PES General Meeting*, pp.1-5, 2015.
[27] W. Dib, G. Kenne and F. Lamnabhi-Lagarrigue, An application of immersion and invariance to transient stability and voltage regulation of power systems with unknown mechanical power, *Proc. of the 48th IEEE Conference on Decision and Control Held Joinly with the 28th Chinese Control Conference*, Shanghai, China, pp.7837-7842, 2009.
[28] X. Jiao, Y. Sun and T. Shen, Adaptive controller design for a synchronous generator with unknown perturbation in mechanical power, *International Journal of Control, Automation, and Systems*, vol.3, no.2, pp.305-314, 2005.
[29] Z. Zhou, Y. Ma, J. Yu, X. Wang and W. Li, Fuzzy approximation-based adaptive discrete-time dynamic surface control for induction motors, *ICIC Express Letters*, vol.11, no.1, pp.231-237, 2017.